REPORT DOCUMENTATION PAGE

Form Approved
OMB No. 0704-0188

1. REPORT DATE *(DD-MM-YYYY)*	2. REPORT TYPE	3. DATES COVERED *(From - To)*
04-06-2010	Technical Paper	

4. TITLE AND SUBTITLE

Modeling of Homogeneous Condensation in High Density Thruster Plumes

5a. CONTRACT NUMBER

5b. GRANT NUMBER

5c. PROGRAM ELEMENT NUMBER

6. AUTHOR(S)
Ryan Jansen (USC); Natalia Gimelshein & Sergey Gimelshein (ERC); Ingrid Wysong (AFRL/RZSA)

5d. PROJECT NUMBER

5f. WORK UNIT NUMBER
23080532

7. PERFORMING ORGANIZATION NAME(S) AND ADDRESS(ES)

Air Force Research Laboratory (AFMC)
AFRL/RZSA
10 E. Saturn Blvd.
Edwards AFB CA 93524-7680

8. PERFORMING ORGANIZATION REPORT NUMBER

AFRL-RZ-ED-TP-2010-274

9. SPONSORING / MONITORING AGENCY NAME(S) AND ADDRESS(ES)

Air Force Research Laboratory (AFMC)
AFRL/RZS
5 Pollux Drive
Edwards AFB CA 93524-7048

10. SPONSOR/MONITOR'S ACRONYM(S)

11. SPONSOR/MONITOR'S NUMBER(S)
AFRL-RZ-ED-TP-2010-274

12. DISTRIBUTION / AVAILABILITY STATEMENT

Approved for public release; distribution unlimited (PA #10271).

13. SUPPLEMENTARY NOTES
For presentation at the AIAA Thermophysics Conference, Chicago, IL, 24-28 June 2010.

14. ABSTRACT

A computational approach to homogeneous nucleation is proposed, based on Eulerian description of the gas phase coupled with a Lagrangian approach to the cluster phase. A continuum, Euler / Navier-Stokes solver VAC is used to model the gas transport, and a kinetic particle solver is developed in this work to simulate cluster nucleation and growth. The new model was found to reproduce well the known theoretical dimer formation equilibrium constants for two gases under consideration, argon and water. Reasonable agreement between computed and available experimental data was found in terminal cluster size distributions in nozzle water expansions in a wide range of stagnation pressures. The proposed approach was found to be orders of magnitude faster than a comparable approach based on the DSMC method.

15. SUBJECT TERMS

16. SECURITY CLASSIFICATION OF:			17. LIMITATION OF ABSTRACT	18. NUMBER OF PAGES	19a. NAME OF RESPONSIBLE PERSON
a. REPORT	b. ABSTRACT	c. THIS PAGE			Dr. Ingrid Wysong
Unclassified	**Unclassified**	**Unclassified**	SAR	15	19b. TELEPHONE NUMBER *(include area code)* N/A

Modeling of Homogeneous Condensation in High Density Thruster Plumes

Ryan Jansen*
University of Southern California, Los Angeles, CA 90089

Natalia Gimelshein† and Sergey Gimelshein†
ERC, Inc., Edwards AFB, CA 93524

Ingrid Wysong‡
Air Force Research Laboratory, Edwards AFB, CA 93524

A computational approach to homogeneous nucleation is proposed, based on Eulerian description of the gas phase coupled with a Lagrangian approach to the cluster phase. A continuum, Euler / Navier-Stokes solver VAC is used to model the gas transport, and a kinetic particle solver is developed in this work to simulate cluster nucleation and growth. The new model was found to reproduce well the known theoretical dimer formation equilibrium constants for two gases under consideration, argon and water. Reasonable agreement between computed and available experimental data was found in terminal cluster size distributions in nozzle water expansions in a wide range of stagnation pressures. The proposed approach was found to be orders of magnitude faster than a comparable approach based on the DSMC method.

I. Introduction

Homogeneous condensation plays an important role in many atmospheric and technological processes, and understanding of its physical mechanisms and dependencies is critical for a number of engineering applications. One of such applications, pertaining to post boost vehicle operations at very high altitudes, is related to thruster plume expansion into surrounding rarefied atmosphere.[1] It is well known that particulates of different kind are the main contributor to sunlight scattering observed in high altitude plumes. The effect of sunlight scattering in plumes in which neither carbon soot nor alumina particles were present, with the specific example of the Apollo 8 translunar injection burn,[2] indicates that particles must be formed in the rapid expansion of the exhaust to rarefied atmosphere, mostly from the condensation of water vapor and other combustion products in the plume.

Condensation in the rapidly expanding flows has been observed experimentally as early as mid-30s,[3] and has been extensively studied in the following decades (see for example Ref. 4 and the references therein). Computational modeling of expanding condensing flows has a shorter, although still a respectable history. In the past, two different approaches have been used to describe homogeneous condensation and, in particular, cluster nucleation (formation of small clusters from monomers) in non-equilibrium environment of rapid expansions. In the first approach, based on the classical nucleation theory (CNT)[5] and equilibrium thermodynamics, the key process is the formation of the smallest stable droplets possible, so-called critical clusters, through unimolecular reactions of cluster growth and decay. The classical theory calculates the condensation and evaporation rates using the Gibbs distributions and the principle of detailed balance, and the nucleation rate is then calculated assuming a steady state condition.[6]

The main principles of the classical nucleation theory in combination with the conventional compressible Navier-Stokes gas dynamic equations were used by a number of researchers to numerically predict multi-

*Undergraduate Student, Astronautical Engineering
†Consultant
‡Branch Chief, Propulsion Directorate

dimensional condensing flows (see, for example, Refs. 7–9). The important part of these models is the creation of cluster nuclei at some critical size that depends on local gas conditions. The nucleation rate is governed by CNT, and droplet growth can be derived on the basis of heat transfer conditions surrounding the droplet (the description of Ref. 10 was used in Ref. 8). Both Lagrangian[8] and Eulerian[7] description of condensed droplets was used in the literature.

An alternative approach to modeling homogeneous condensation, is based on some assumed shape of the droplet size distribution function, usually lognormal. In Ref. 11, this assumption is coupled with the a modified form of the Hertz-Knudsen equation, which gives a droplet-gas mass transfer rate as the difference between incoming fluxes from the gas phase and evaporative fluxes from the droplet; a standard Eulerian description was used to model the two-phase flow. In Ref. 12, viscous compressible reduced Navier-Stokes equations[13] are used for the gas phase, while polydisperse particle behavior is described by an Eulerian aerosol moment model which accounts for particle transport due to convection, diffusion, inertia and thermophoresis, as well as particle dynamics due to coagulation, nucleation and condensation. Yet another numerical approach, which uses many of the CNT assumptions, and has been applied mostly to turbulent condensing flows, is based on a semi-Lagrangian treatment of droplets.[14,15] Semi-Lagrangian methods combine both Eulerian and Lagrangian points of view: a scalar field is discretized on a Eulerian grid, but is advanced in time using a Lagrangian technique.

While different methods were applied to predict cluster nucleation and growth in gas flows, most of the researchers that used the classical nucleation theory applied an Eulerian approach to the gaseous phase, usually based on the solution of full or reduced Navier-Stokes equations. A different strategy was proposed in Ref. 16, where a particle-based direct simulation Monte Carlo (DSMC) method[17] was used to compute the gas flow. A Lagrangian technique was applied to model cluster evolution. Similar to Ref. 7, new clusters were created at a critical size, and their further growth was calculated with the CNT approach.

Some important assumptions of the CNT, such as unimolecular reactions of cluster growth and decay and the use of the principle of detailed balance that implies thermodynamic equilibrium, limit its applicability as a prediction tool for highly non-equilibrium flows, such as rapidly expanding plumes. In such flows, the impact of thermal non-equilibrium between gas and particles is expected to significantly impact the growth rates and cluster size distributions. Moreover, the cluster size distribution may have a significantly more complex shape than the lognormal distribution often used in the literature. An illustrative example of such complex distributions was provided in Ref. 18, where the terminal cluster size distributions were measured in water and ammonia expansions for a wide range of stagnation pressures and temperatures; the results were obtained by doping the water and ammonia clusters by one Na atom, which was photoionized close to the threshold without fragmentation.

The experimental study[18] showed that for lower pressures, the size distribution is exponential; for higher pressures, the size distribution approaches the lognormal profile, and for intermediate pressures, it was a complex bi-modal shape. The transition from the exponential to bi-modal shape was explained by changing governing mechanisms of cluster growth. For lower pressures, the clusters grow mostly through monomer sticking, while at higher pressures, the main mechanism is cluster-cluster collisions and coalescence. The bimodal shape of the cluster size distribution function for intermediate plenum pressures was attributed in Ref. 18 to the processes of coalescence of small particles (such as dimers and trimers) on larger clusters and of coagulation of larger clusters. A bimodal distribution of cluster sizes was measured[18] for a number of chamber pressures, varied by up to an order of magnitude; typically, it was observed when the average cluster size was from below 100 to about 1000. These cluster sizes are believed to be largely occurring in a number of applications, including rocket thruster plumes.

The inability of CNT based methods to accurately predict the cluster size distributions in strongly nonequilibrium flows dictates the use of the second approach, known as the kinetic approach, which treats nucleation as the process of kinetic chemical aggregation.[19] Unlike CNT, the kinetic approach does not assume local thermodynamic equilibrium. Instead, a microscopic process of the interactions of monomers and clusters is described either analytically via a mathematical model, e.g., by the Smoluchowski equations where the interaction between particles is modeled by the reaction rates,[20,21] or in computer simulations, e.g., in molecular dynamics calculations where the interaction is modeled by an interaction potential.[22,23] It is well known that the application of either the Smoluchowski equations or the molecular dynamics approach to the modeling of cluster evolution in multi-dimensional thruster plume flows is computationally unfeasible.

A more promising direction in modeling rapidly expanding condensing flows is the use of the DSMC method. As a numerical approach to the Boltzmann equation, it is applicable to a large range of flow condi-

tions. In this method, cluster-cluster and cluster-monomer interactions including the multi-body reactions of cluster nucleation can be seamlessly incorporated. Over the last several years, the DSMC method has been extensively and successfully applied to modeling the processes of cluster formation and evolution in supersonic jets.[24,25] The work of these authors[26] extended the kinetic dimer formation approach of Ref. 27, who assumed that a ternary collision always results in a dimer formation, to include molecular dynamic (MD) simulations for obtaining information on the probability of dimer formation in such ternary collisions. The work[28] used a temperature-dependent probability of formation of argon dimers. Another DSMC-based model, which treats both cluster nucleation and evaporation (RRK[29] technique was used for the latter) from the principles of the kinetic theory, was introduced in Ref. 30.

The downside of using the DSMC method as the modeling approach for condensing plumes is its high computational cost. It may be applied to relatively low density plumes, when the typical size of clusters does not exceed 100-mers. For higher pressures, this approach becomes prohibitively expensive. The most serious numerical limitation of the DSMC method is related to the fact that a large number of simulated particles has to be computed. The required number of simulated particles generally increases as n^2 for 2-D problems, and n^3 for 3-D problems, where n is the gas density. Most of the simulated particles are monomers; the statistical scatter for cluster species is therefore extremely high as compared to the monomers. The use of species weights in the DSMC method is questionable, since clusters, especially for larger pressures, are not a trace species, and thus strongly impact the flow properties through the heat release during the nucleation and cluster growth process.

The main objective of this work is the development of a new method, that would combine the computational efficiency of an Eulerian continuum approach and the physical accuracy of a Lagrangian kinetic approach. The proposed method integrates an Eulerian approach for monomer gas flow based on the solution of Navier-Stokes equations, with a Lagrangian approach for clusters based on a DSMC-like particle-based algorithm. The work is built on the previous effort[30] where the first-principles model of homogeneous condensation was formulated, and all of the most important processes of cluster nucleation and evolution were considered at the microscopic level. The processes included in the model[30] are (i) creation of dimers through the collision stabilization of collision complexes, (ii) elastic monomer-cluster collisions that change the translational and internal energies of colliding particles, (iii) inelastic monomer-cluster collisions that result in monomer sticking, (iv) cluster-cluster coalescence, (iv) evaporation of monomers from clusters. All these processes are present in the new method. In the next sections, the details of the method are discussed, and the homogeneous nucleation rates in argon and water thermal bath environments are analyzed, followed by the validation study that focuses on comparison of cluster growth in plumes with available experimental data on terminal cluster size distribution.

II. Numerical approach

The main idea of the present numerical method is to calculate gas flow solving the compressible Navier-Stokes equation, model the nucleation process starting from the dimer formation and up using the elementary kinetic theory for cluster-cluster and cluster-monomer collisions, and and exchange the information between the continuum and kinetic parts of the simulation through source terms, so that these parts are fully coupled. Similar to the DSMC method, a finite number of simulated clusters replace the real ones, so that each simulated cluster represents a large number of real particles.

A. Eulerian approach to gas phase

The Eulerian-Lagrangian approach with a two-way coupling developed in Ref. 31 to model two-phase plume flows represents the computational framework of the new condensation model. Gas properties are computed using an Eulerian approach based on the solution of the Navier-Stokes equations with appropriate source terms that take into account the impact of condensation process and clusters on the gas flow,

$$\frac{D\rho}{Dt} + \rho(\bigtriangledown \cdot \mathbf{V}) = M,$$

$$\rho\frac{D\mathbf{V}}{Dt} - \bigtriangledown \cdot \Pi_{ij} = D_i,$$

$$\rho\frac{D\mathbf{V}}{Dt} \cdot \mathbf{V} + \bigtriangledown p \cdot \mathbf{V} - \bigtriangledown \cdot \tau_{ij}) \cdot \mathbf{V} = Q,$$

where M, D_i, and Q are the corresponding mass, momentum, and energy source terms that define the impact of condensation on gas molecules.

The Navier-Stokes equations are solved using Versatile Advection Code (VAC)[32] modified to include the above particle source terms. Particle properties are determined by Lagrangian tracking of particles through the gas flowfield and statistical averaging of particle parameters. For the gas phase, an explicit time integration is used, and the Navier-Stokes equations are solved using the TVD-Lax-Friedrichs scheme with minmod limiter. For the particle phase, a fourth order Adams-Moulton method is used to integrate particle equations of motion.

In the current implementation, the clusters are assumed to be in the translational equilibrium with gas, that is, their macroscopic velocity and translational temperature are assumed to be equal to the corresponding parameters of the gas. At each time step Δt, the clusters are moved by $\mathbf{v}_i \Delta t$, where $\mathbf{v}_i$ is the velocity of the i-th cluster. Then, the cluster collision relaxation processes are modeled at the kinetic level. These processes, that include the formation of new dimers, monomer-cluster collisions that involve energy transfer between internal and translational modes of colliders, cluster-cluster coalescence, and cluster growth and shrinking due to monomer sticking and evaporation, are described in detail below. After the cluster relaxation processes, the changes in cluster mass and internal energy is evaluated, and then used to calculate the RHS of the Navier-Stokes equations.

B. Lagrangian approach to cluster formation and evolution

Replacing the kinetic modeling of gas transport with a continuum approach is justified by the proximity to equilibrium of velocity distribution functions of gas molecules in condensing plumes, where the gas density is fairly large, and mean free path is many orders of magnitude smaller than the characteristic flow size (usually nozzle throat or exit diameter). The cluster nucleation and evaporation processes, though, require kinetic treatment for a number of reasons, most notably non-equilibrium cluster size distribution and the departure from equilibrium of cluster internal energies. Such a kinetic, Lagrangian treatment is therefore proposed in the present work. Although the Lagrangian approach to modeling cluster nucleation follows to some extent the first-principle, fully kinetic approach of the previous work,[30] it has a number of key differences, mostly related to the fact that monomers are simulated at the continuum level, and thus some approximation has to be used to include cluster-related collisions that involve monomers.

1. Dimer formation

Dimers are formed as a result of a collisional stabilization of collision complexes consisting of two monomers that collide with third particles during their life time; the third particle is needed to carry away extra energy and thus stabilize the dimer. In each stabilization event, there is also an energy release from the potential levels of two monomers that formed the collision complex, to the internal energy modes of the newly created dimer and the third particle, and the translational modes of their relative motion.

The change in the dimer number density as a result of new dimers formed in each cell over a single time step Δn_d is calculated from the known recombination rate and macroscopic gas properties in the cell as follows

$$\Delta n_d = K_{rec} n^3 \Delta t. \tag{1}$$

Here, K_{rec} is the recombination rate and n is gas number density. Then, the number of newly created dimers is given by $\frac{\Delta n_d V_c}{F_{num}}$, where F_{num} is the number of real clusters represented by one simulated cluster (similar to F_{num} traditionally used in the DSMC method) and V_c is the cell volume. Generally, any form of temperature dependence may be used to define K_{rec}; in this work, a temperature dependence similar to the well known Arrhenius dependence is used, $K_{rec}(T) = A \times B^T \exp(-CT)$. In this equation, constants A, B and C may be chosen either from values known in the literature, or selected to reproduce analytical dimer formation equilibrium constants.

The initial position of each formed dimer is selected uniformly within the cell, its initial velocity is set equal to the macroscopic velocity of the gas in the cell, and the initial cluster internal energy is sampled as follows. First, the total available energy in the collision complex-third particle collision is assumed to be equal to

$$E_{tot} = \left(\frac{3}{2}\xi_{int} + \frac{4 - 2\alpha_m}{2} + \frac{4 - 2\alpha_c}{2} \right) kT, \tag{2}$$

where ξ_{int} is the number of internal degrees of freedom of the monomer (zero if atom), and α is the VHS model parameter. In this expression, the $4-2\alpha_m$ term corresponds to the number of relative translational degrees of freedom in the monomer-monomer collision, and α_m corresponds to this type of collision. Similarly, $4-2\alpha_c$ is the number of relative translational degrees of freedom in the collision complex-monomer collision. After that, the total energy is increased by evaporation (dimer dissociation) energy E_{evap}, and then split between the newly created dimer and the third particle using the Larsen-Borgnakke (LB)[33] procedure. This procedure, initially developed to model energy transfer between translational and rotational modes of colliding molecules, is based on the assumption that after-collision relative translational and internal energy modes will be populated according to the local equilibrium distribution functions. In this work, the energy transfer was assumed to include all available energy modes, i.e. energy of relative motion of the dimer-monomer pair, the internal energy of the monomer, and the internal energy of the dimer. For monomers, only rotational modes are assumed to be exited, since at low gas temperatures in expanding plumes (below 300 K in this work) the excitation of vibrational modes is negligible. The number of internal degrees of the dimer is calculated from the dimer heat capacity C_v

$$\xi^{int} = n\frac{2C_v}{k} - 3, \tag{3}$$

where n is the number of monomers in the clusters ($n = 2$ for dimer). Note that this expression is also utilized for larger clusters. The values of heat capacities used in this work for argon and water clusters are taken from Ref. 30.

The dimer formation procedure thus results in the formation of dimers at a given temperature dependent rate, and each of these dimers is characterized by unique internal energy that is then used in the cluster collision and evaporation processes.

2. Inelastic monomer-cluster collisions

The interaction between monomers and clusters is an important process that results in energy transfer between the internal energy modes of clusters and translational modes of colliders. The change in the cluster internal energies greatly impacts the evaporation rates, and thus needs to be properly modeled. It was pointed out in Ref. 30 that when the LB model is used to simulate the energy transfer in monomer - cluster collisions, it is reasonable to introduce an inelastic collision relaxation number Z, which defines the probability that a cluster will experience an inelastic collision leading to a change in its internal energy in a single collision as $P_i = \frac{1}{Z}$. This means that only every one out of every Z collisions of a cluster will lead to the change in its internal energy. In every collision that involves such a change, the after-collision energies are selected according to the local equilibrium distribution functions. It is thus similar to the rotational and vibrational relaxation numbers Z_r and Z_v widely used in the DSMC method. The values of Z were chose[30] to provide good agreement with known theoretical dimer formation equilibrium constants for argon and water.

A similar approach is used in the present model, with one significant exception. Among many monomer-cluster collisions, only those that cause the cluster internal energy change are important in terms of cluster evolution, and thus only those collisions were modeled. Since the value of Z is typically larger than one (for example, for water it is 10 for temperatures between 100 K and 300 K), such an approach allows for significant reduction in computational time. The approach therefore is reduced to the analysis of each cluster in the computational domain in terms of possible inelastic collisions with monomers as follows.

First, note that the probability that a cluster will experience an inelastic collision leading to a change in its internal energy during time τ is equal to $p = 1 - \exp(\nu\tau/Z)$, where ν is collision frequency. Time to the next inelastic collision can be sampled as $\tau_{ie} = -\log(\Re)Z/\nu$, where $\Re$ is a random number uniformly distributed between 0 and 1. The algorithm to model inelastic collisions for a given cluster over time step Δt is thus

1. Set t_{local} to 0
2. Calculate ν and Z as functions of gas macroparameters
3. Change $t_{local} = t_{local} - \log(\Re)Z/\nu$
4. If $t_{local} > \Delta t$, go to the next cluster

5. Perform inelastic collision.

6. Go to step 3

Unlike Ref. 30, where the kinetic, microscopic information on monomers that includes their individual energy states and velocities is available, the present method provides only the macroscopic information such as temperature and number density. While sufficient to calculate the local collision frequency and temperature-dependent internal energy relaxation number Z, this is not enough to simulate monomer-cluster collisions (Step 5) at the kinetic level. In order to do that, an additional information about the velocity and energy distribution functions of monomers is necessary. In this work, the internal energy of the colliding monomer and the relative translational energy of the colliding monomer-cluster are sampled from the corresponding equilibrium distributions. The total collisional energy, which is a sum of these two energies and internal energy of the cluster, is then redistributed between the relative translational and the internal modes of the cluster and the monomer using the LB model. The numbers of the corresponding degrees of freedom are defined as described in the dimer formation section.

3. Cluster growth and evaporation

The key processes that determine small cluster evolution is sticking and evaporation of monomers off the clusters. In order to drastically reduce the requirements to the minimum time step used in the simulation, and provide accurate account of evaporation and sticking events of a single cluster, the growth and evaporation processes are combined in a single algorithm as follows.

The cluster sticking rate is calculated as $\nu_s = nP_s\langle\sigma_c g\rangle$, where P_s is the probability that a monomer will stick to the cluster after the collision, σ_c is monomer-cluster collision cross-section calculated using the hard sphere model, and g is relative collision velocity. In the hard sphere model, where the collision cross section is written as πd^2, the collision diameter d is written as the average of the diameter of the colliding monomer taken from the VHS model[17] and the cluster diameter obtained through an empirical correlation used extensively in the past (see, for example, Ref. 16),

$$d_c = 2 \cdot (A \cdot i^{\frac{1}{3}} + B), \tag{4}$$

where A and B are species-dependent constants, and i is the number of monomers in the cluster. In this work, the values of A and B were 2.3×10^{-10} m and 3.4×10^{-10} m for argon,[24] and 1.9×10^{-10} m and 2.4×10^{-10} m for water.[34]

For monomer-cluster sticking collision probability, an empirical dependence of the probability on the species diameter d and mass m given in Ref.[35] is used, that may be written as

$$\epsilon = \frac{d_N^2}{(d_N + d_1)^2} \left(\frac{m_N}{m_N + m_1} \right)^{\frac{1}{2}}, \tag{5}$$

where indices N and 1 refer to the cluster of a size N and monomer, respectively.

To evaluate the rate of evaporation of monomers off the cluster surface, the RRK model[29] is used, similar to Ref. 30. Following Ref.,[36] the evaporation rate k_e is calculated as

$$k_e = \nu N_s \left(\frac{E_{int} - E_{evap}}{E_{int}} \right)^{3N-7} \tag{6}$$

Here, N is the number of monomers in the cluster, ν is the vibration frequency, N_s is the number of surface atoms, E_{evap} is the evaporation energy, and E_{int} is the cluster internal energy. For dimers, the exponent $3N - 7$ is replaced with 1. The number of surface atoms N_s is N for $N < 5$, $N - 1$ for $4 < N < 7$, and $(36\pi)^{1/3}(N^{1/3} - 1)^2$ for $N > 6$. The vibration frequency was taken to be 2.68×10^{12} s^{-1} for water clusters,[37] and 10^{12} s^{-1} for argon clusters.[36]

With the evaporation and sticking rates defined by the above expressions, the following algorithm is used to model sticking and evaporation processes.

1. Set t_{local} to 0.

2. Calculate sticking and evaporation rates ν_s and nu_e

3. Change $t_{local} = t_{local} - \log(\Re)/(\nu_e + \nu_s)$

4. If $t_{local} > \Delta t$, proceed to the next cluster

5. If $\Re > \nu_s/(\nu_s + \nu_e)$, increase cluster size by one monomer (see below)

6. Otherwise, evaporate one monomer (see below). If, after evaporation, the cluster becomes a monomer, remove this cluster from the simulation and proceed to the next cluster.

7. Return to step 2

For cluster growth, the monomer internal energy and relative translational energy are sampled from the corresponding equilibrium distributions, and the after-sticking cluster internal energy is equal to the sum of cluster pre-collisional internal energy, internal energy of the monomer, relative translational energy, and evaporation energy E_{evap}.

For cluster evaporation, the cluster internal energy is decreased by E_{evap}, and the remaining energy is redistributed between the cluster internal modes, internal modes of the departing monomer, and relative translational modes using the LB model. Note here that only cluster internal energy is calculated, while the cluster velocity and monomer properties are assumed to accommodate to the gas properties.

4. Cluster-cluster collisions

The cluster-cluster collisions is an important process that has to be taken into account for accurate description of cluster evolution, since it is the key factor determining the size distribution of larger clusters. Cluster-cluster collisions have different outcomes which generally may be classified as coalescence and reflexive and stretching separations. The dynamics of water droplet collisions for macroscopic particles was studied experimentally in Ref. 38 where the boundaries between both of the separating collisions and coalescence collision were examined as a function of the size ratio and the Weber number in the wide range of Weber numbers from 1 to 100. For microscopic particles with sizes from dimers to thousand-mers, the authors are not aware of any comparable to Ref. 38 systematic study where the results of cluster collisions would be analyzed for different Weber numbers. Extrapolating the results of Ref. 38 to microscopic particles of interest in this work, one can notice that for typical plume temperatures on the order of 100 K and thus Weber numbers on the order of the unity or less, the clusters would mostly experience coalescence and not separation. However, such an extrapolation, although partially justified for hundred- and thousand-mers, is much more questionable for smaller clusters, where more reflexive collisions may be expected. In this work, in the absence of reliable size and relative velocity dependence of the collision outcome for small clusters, a constant coalescence probability is assumed.

The cluster-cluster collisions are modeled using a conventional DSMC algorithm. The majorant frequency scheme[41] of the DSMC method was utilized for this purpose. At every time step, the current maximum cluster size is obtained in each cell. Then, the majorant collision frequency is calculated based on this maximum cluster size and maximum relative collision velocity evaluated from the local gas temperature. The majorant collision frequency is then multiplied by the coalescence probability, since only the coalescence events are modeled (reflexive separation is believed to have negligible effect on cluster properties, and the stretching separation process is not included in the present model). After a pair of clusters K and L is selected for physical collision, the coalescence event is modeled, with the result being a larger cluster M with mass m and internal energy E_{int} calculated from the properties of colliding clusters using the mass and energy conservation constraints. The laws dictated

$$m_M = m_K + m_L, \quad E_{int,M} = E_{int,K} + E_{int,L} - Q,$$

with $Q = -Q_M + Q_K + Q_L$, where Q_i is the energy of vaporization of cluster i.

After all collision and evaporation processes are simulated for a given time step, the mass and energy change over this time step are calculated over all cells in order to be included in the Eulerian gas flow equations. The primary purpose of this step is accurate conservation of all conservative properties in the simulation.

III. Thermal Bath Relaxation

Inelastic cross sections for monomer-monomer and monomer-cluster collision mechanics are needed as part of a comprehensive validation of a kinetic condensation model. These cross sections, in general a function of the translational and internal energy states of pre- and post-collision particles, are unavailable for the species and temperatures desired. However, equilibrium rates for nucleation and evaporation for both water and argon are available in literature. Furthermore, a necessary condition for the model to fulfill is that it produces correct behavior in equilibrium, although it does not guarantee the model will have correct nonequilibrium behavior.

Such equilibrium behavior was modeled in this work by a thermal bath relaxation of both argon and water at various temperature conditions. The equilibrium constants for the formation of clusters were calculated and compared to published results of Refs. 39,40. In addition, they were compared to the previously obtained results of the DSMC based model.[30]

To model argon equilibrium, over 10 million simulated particles were used, and the run was allowed to run until a steady equilibrium value was reached, usually about half a million time steps. The timestep for argon was selected to be 8×10^{-11} s, so that there were much fewer than 1 collision per molecule per timestep, making the results independent of step size. Number density of 10^{22} m^{-3} was selected to ensure that clusters made up less than 0.1% of the gas, while maintaining the 10 million particle requirement. This ensured that adequate numbers of particles were present for statistics, and that the clusters did not have a significant impact on the behavior of the gas.

The dimer formation rate k_{rec} for argon was computed using the stable dimer formation rate from Ref. 39, that is written as

$$k_{rec} = A \times B^T \exp -CT \tag{7}$$

The values of A, B, and C given in Ref. 39 are $A = 10.15 \times 10^{-44}$ m^6·molec^{-2}· s^{-1}, $B = -0.278$ and $C = 3.10 \times 10^{-3}$ K^{-1}.

The argon equilibrium rate as a function of temperature is shown in Fig. 1. It is compared with the DSMC results from Ref. 30. There is good agreement between this model and the DSMC results, which were shown to agree with several experimental results. However, there is a breakdown in agreement at higher temperatures where the present model sharply under-predicts the equilibrium constant. The reason for good agreement at lower temperatures is that the temperature dependence of the inelastic collision number Z was chosen to allow this to fit well. However, the under-prediction at higher temperatures occurs regardless of the value of Z chosen. This is acceptable for this work, as the temperatures of further interest all fall within the range of good agreement.

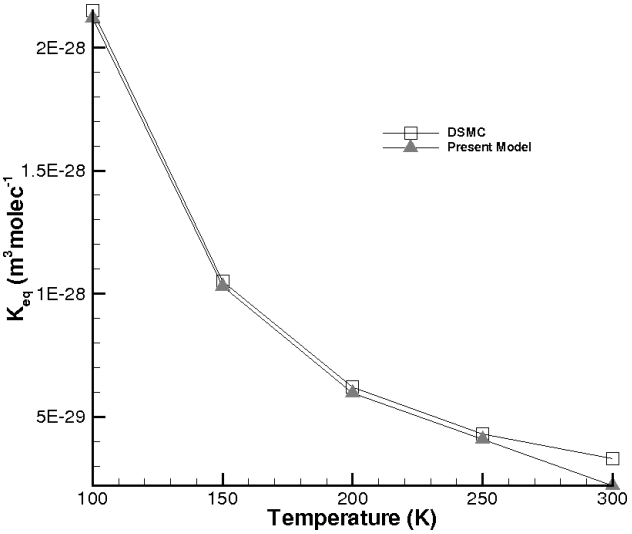

Figure 1. Argon dimer equilibrium rate as a function of gas temperature.

In modeling water equilibrium, about 1 million simulated particles were used, and the process was again

allowed to run until a steady equilibrium was reached, about half a million timesteps. The timestep was set at 1×10^{-7} s, which ensured that there were still much fewer than one collision per particle per timestep, but also that the system would reach complete equilibrium within a reasonable number of timesteps. Similar to argon, number density of 10^{21} m^{-3} was selected to ensure that clusters were less than 0.1% of the gas while maintaining 1 million simulated particles. Due to the low fraction of clusters, this ensured the behavior of the gas was not influenced by the presence of the clusters. Note that using a smaller gas density does not change the results of the simulations.

The water equilibrium rate is shown in Fig. 2. It is compared with the theoretical predictions.[40] There is good agreement between the current model and the results of Ref. 40 at all temperatures investigated in this work. Furthermore, the parameter Z has relatively small effect on the equilibrium rate for water.

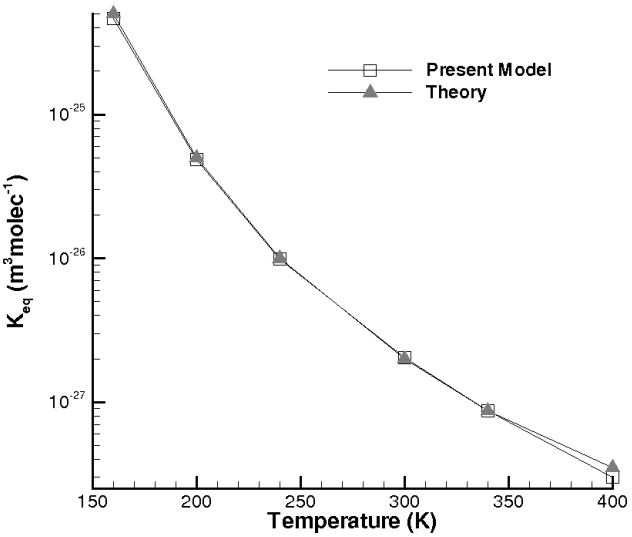

Figure 2. Water dimer equilibrium rate as a function of gas temperature.

The parameter Z, or inelastic collision number is effectively the inverse probability of the energy transfer between the internal modes of a dimer and the translational modes in the dimer-monomer collisions, was found to be an important factor influencing the magnitude of the equilibrium constant. A possible explanation is as follows. The dimers are formed after three-body collisions, and typically have internal energies smaller than the evaporation energy after those collisions. In argon, the evaporation energy for a dimer is small compared to the typical total collision energy for all the temperatures under consideration. ($E_{evap}/k \approx 140$ K). This means most dimers have an internal energy in excess of the evaporation energy after only a couple inelastic collisions with monomers for thermal bath temperatures greater than 140 K. With an internal energy larger than the evaporation energy, the lifetime of these dimers is very short, about a picosecond. This means the dimer-monomer energy transfer is the main contributor to quick dimer dissociation. It is important to note that Z has little impact on dimer formation, and only affects the evaporation rates. Therefore, in the range of temperatures of interest, the equilibrium constant for argon was found to be nearly proportional to Z^{-1}, except for at high temperatures.

For water, the equilibrium constant in much less dependent on Z. This is because the evaporation energy of a dimer is much larger than the translational energy of colliding molecules and dimers. For example, the reduced evaporation energy for water is $E_{evap}/k \approx 1,800$ K, while the gas temperatures were on the order of 300 K. Therefore, K_{eq} for water is much less dependent on Z, and is effectively independent of its value.

IV. Water cluster size distribution in nozzle expansion

The second part of the validation and numerical analysis of the presented condensation model is focused on the nucleation and evolution of small water clusters in a conical nozzle. The study was prompted by the availability of high quality experimental data[18] on terminal size distribution of water clusters in the wide range of flow conditions where the cluster size distribution changes its shape from exponential at low

pressures to bimodal at intermediate pressure to lognormal at high pressures. The experimental results were obtained by doping the water clusters by one Na atom, which is photoionized close to the threshold without fragmentation. The nozzle is a conical nozzle with a 41° opening angle, a total length of 2 mm, and a throat diameter of 50 μm. Four different stagnation pressures were computed, considered in Ref. 18, 1.577 bar, 2.173 bar, 5.144 bar, and 8.307 bar, with the corresponding stagnation temperature of 495 K. Since the background pressure effect in the experiment is believed to be small,[42] the flow expansion into the vacuum is modeled.

The computations were conducted on a 500×150 spatial grid, with cell sized reduced in radial direction and increased in the axial direction. An adiabatic nozzle nozzle wall condition was used, although previous studies have found that there is no impact of the wall condition on the coreflow were the cluster sizes are recorded. The number of simulated droplets was about 500,000, which was found to provide adequate statistical accuracy for the calculations. The particles were assumed to condense on the nozzle surface. Uniform inflow conditions were imposed at the nozzle throat, calculated from the isentropic flow relations. To compare the cluster size distributions with the terminal distributions[18] measured far downstream from the nozzle, the computed the size distributions in several stations along the nozzle axis were analyzed to provide distance-independent distributions. The domain size was increased in the axial direction from 4 mm for the lowest pressure to 20 mm for the highest pressure to ensure that the size distributions at the exit boundary are essentially frozen.

Typical run time for the lowest pressure under consideration was several hours, and for the highest pressure was up to two days on a single processor computer. Comparing these numbers with those of Ref. 30 where a DSMC method was used to model a 1.577 bar water expansion, the new approach is about 50 times faster than the DSMC based one for the lowest pressure, and this factor will grow significantly with pressure. The reduction in speed is mostly related to the time efficient modeling of gas transport with a continuum method. Since clusters comprise only a relatively small fraction of the particles in the flow, gas transport modeling is the most time consuming part of any DSMC-based technique. Note that species weights for cluster species would reduce the time requirements of a DSMC-based condensation model, but the application of weights is questionable in condensing flows since the condensation significantly changes the gas flow.

Consider first the gas and particle properties along the nozzle axis. The gas translational temperature for the lowest and highest pressures under consideration is shown in Fig. 3. Here, X=0 corresponds to the nozzle throat. As expected, the water nucleation results in noticeable increase in gas temperature due to evaporation heat release. For the 1.577 bar case, the temperature in the plume region is up to 30 K higher when the condensation is included, which is comparable to the magnitude of the temperature in the non-condensing flow. Note a small temperature increase at about 0.25 mm is related to the compression wave that originates near the nozzle throat and propagate to the nozzle axis. It presents both in the condensing and non-condensing flow, and the location is nearly the same since the impact of the condensation is not very significant at this point.

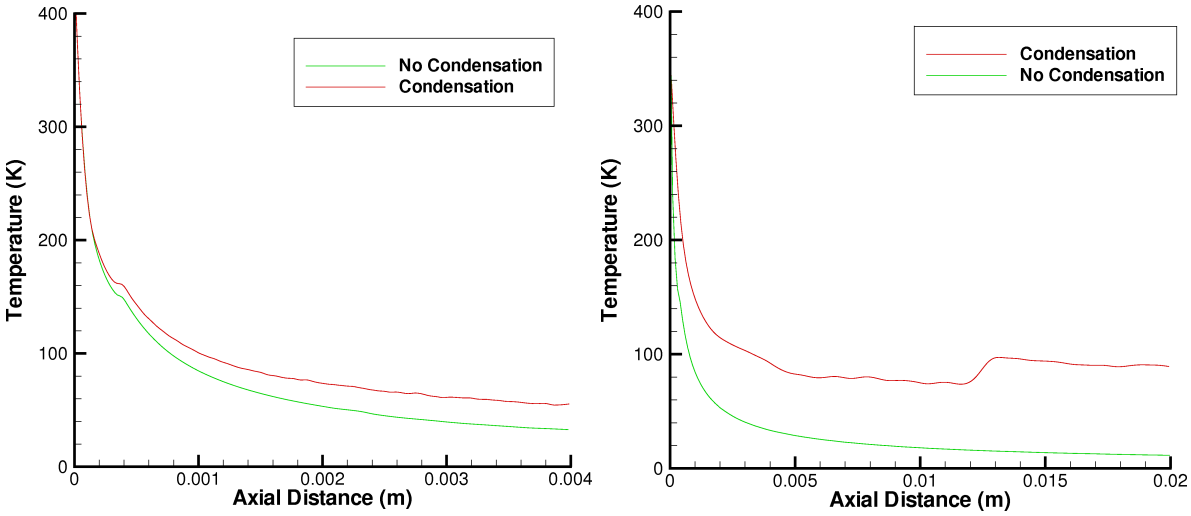

Figure 3. Gas temperature profile along the nozzle axis for $p_0 = 1.577$ bar (left) and $p_0 = 8.307$ bar (right).

For the 8.307 bar case, the influence of the condensation is obvious almost immediately after the nozzle throat (the temperatures start to deviate after the first 100 μm from the throat), and in the plume the gas temperature is several times higher in the condensing flow. Note some statistical scatter seen in this figure, where instanteneous gas properties are presented (an interpolation procedure was used here to smooth the results). The instanteneous properties are dependent on current cluster properties, and the use of a finite number of simulated clusters contributes to their scatter. The higher temperatures in the nozzle for the condensing flow cause the formation of a compression wave near the nozzle lip, that propagates downstream and reflects at the axis at X≈12 mm. This results in a significant rise in gas temperature.

Consider now the terminal cluster size distributions at different stagnation pressures. Note first that there are several important properties that strongly affect the size distributions, among which are the evaporation heat, heat capacity, monomer sticking and cluster coalescence probabilities. The first two of these properties are mostly functions of the cluster size, and the latter two, being characteristics of binary collisions, depend on the cluster sizes, internal energies, and relative collision velocities. The use of a constant coalescence probability in this work is a significant oversimplification of the actual cluster collision process, primarily related to the lack of information on collisions of small clusters. While the coalescence probability of two relatively large clusters (100-mers and larger) may be reasonably assumed to be close to the unity for Weber numbers on the order of 1, the coalescence of smaller clusters is less likely and for the limiting case of dimer collisions may approach that of monomer sticking, which is about 0.2 for water.

The numerical analysis has shown that the size distribution significantly depends on the coalescence probability, as shown in Fig. 4. The increase in the coalescence probability from 0.25 to 1 results in significant redistribution of cluster sizes and shift from smaller sizes to larger ones. Such a trend is expected, since higher coalescence probability at a given collision rate increases the population of large clusters. Although the coalescence is accompanied by energy release from the electronic structure of smaller clusters to the internal energy of larger clusters, the larger internal energy is then redistributed over a significantly larger number of internal degrees of freedom. The resulting gas temperatures were therefore found not to change noticeably with the coalescence probability.

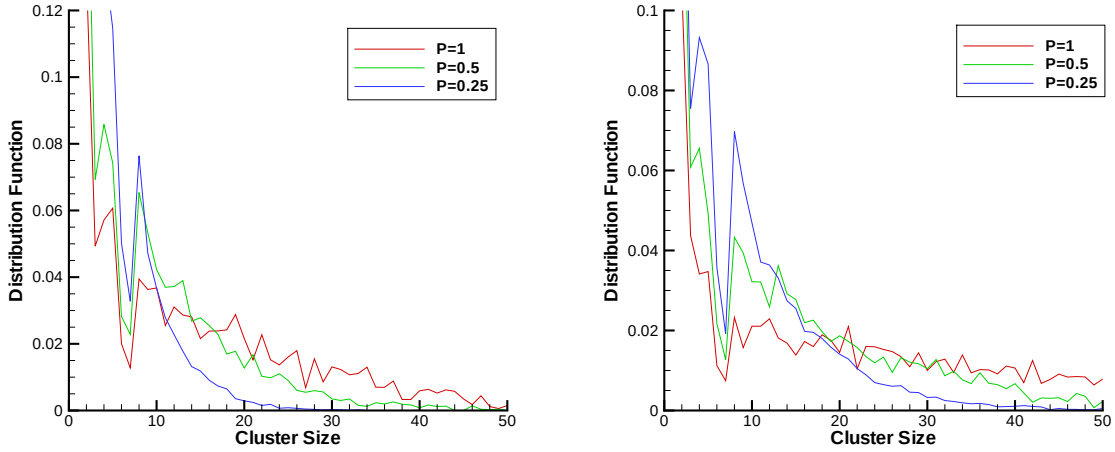

Figure 4. Computed cluster size distributions for different coalescence probabilities P at $p_0 = 1.577$ bar (left) and $p_0 = 2.173$ bar (right).

Comparison of the computed and experimental cluster size distributions[18] for these pressures is presented in Fig. 5. Since the dimers were not measured in Ref. 18, hereafter the experimental points were normalized to match the population of the computed clusters excluding dimers. The case with a coalescence probability of 0.5 gives better agreement with the data, and is therefore shown here. It needs to be mentioned here that a local minimum observed for 6-mers and a local maximum observed for 8-mers is not a statistical fluctuation, but the consequence of the corresponding minimum and maximum in the cluster evaporation energies. Note that for $p_0 = 1.577$ bar, the best agreement with the data would produce a computation that utilizes a constant coalescence probability between 0.25 and 0.5, whereas for $p_0 = 2.173$ bar, a larger coalescence probability between 0.5 and 1.0 would produce a better agreement. This is reasonable, since

higher pressures are generally characterized by higher degree of nucleation and larger cluster sizes, for which the coalescence probability is expected to increase.

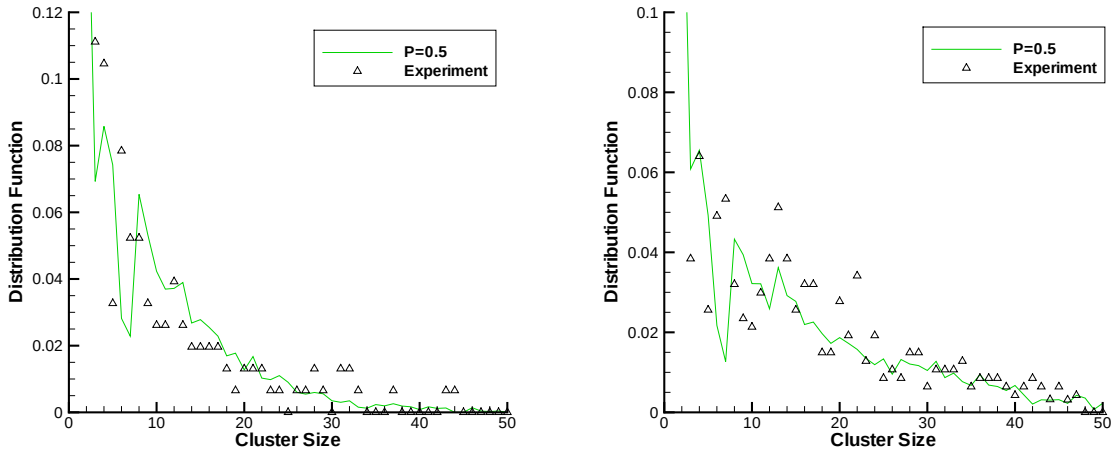

Figure 5. Terminal cluster size distributions for $p_0 = 1.577$ bar (left)and $p_0 = 2.173$ bar (right): comparison with data.[18]

For the two largest pressures under consideration, the computations with a coalescence probability of 1 provide better agreement with the data, and the corresponding results are shown in Fig. 6. For $p_0 = 5.144$ bar, the computed location of the second maximum in the distribution function agrees well with the corresponding experimental value, although the population of such clusters is somewhat higher in the experiments. The most noticeable difference is observed in the large cluster tail, where clearly more clusters were observed in the experiment. In the calculation, the large cluster tail is closer to the lognormal shape. Interestingly, the situation is opposite for $p_0 = 8.307$ bar, for which the tail is somewhat more populated in the numerical prediction. More importantly, the numerical results do not produce a clear bimodal structure at this pressure. Although this is clearly related to some approximations used in the model, more research is needed to single out the most important reason for this. The average cluster sizes for the above computation vs experiment comparisons are summarized in Table IV. There is a reasonable agreement between the results, especially for the three lowest pressures.

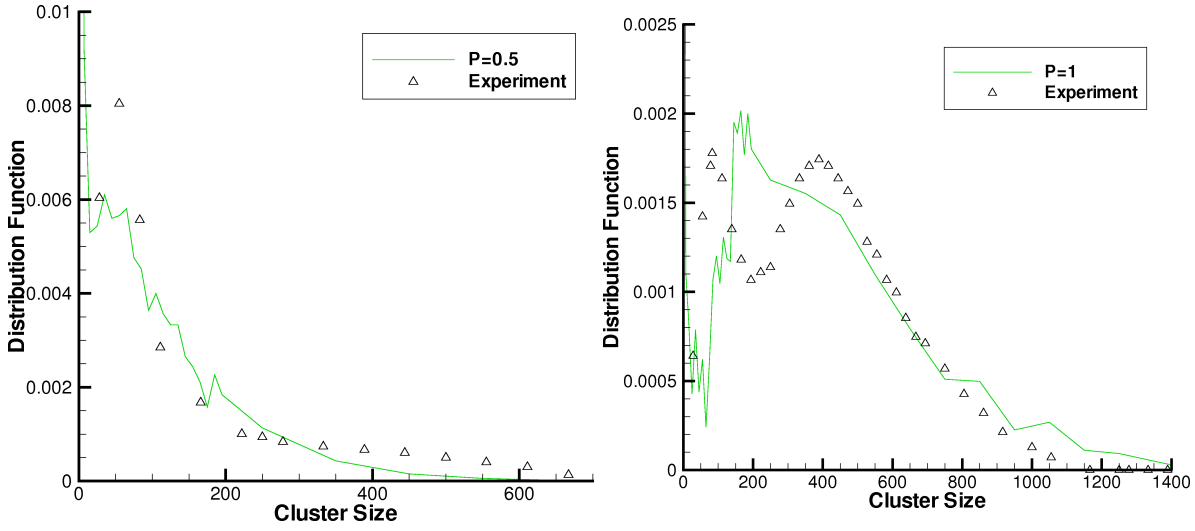

Figure 6. Terminal cluster size distributions for $p_0 = 5.144$ bar (left)and $p_0 = 8.307$ bar (right): comparison with data.[18]

Stagnation pressure, bar	Computation	Experiment
1.577	12	9
2.173	18	20
5.144	107	80
8.307	417	338

Table 1. Averate computed and measured cluster sizes at different pressures.

V. Conclusions

New method for modeling homogeneous condensation is presented, based on Eulerian description of gas phase coupled with a Lagrangian approach to the cluster phase. A continuum, Euler / Navier-Stokes solver VAC is used to model the gas transport, and a kinetic particle solver is developed in this work to simulate cluster nucleation and growth. The conservation of properties is enforced through a two-way coupling, with gas properties influencing the cluster evolution through the dimer formation and monomer-cluster collisions (both elastic and inelastic), and mass, momentum, and energy transfer from the cluster to the gas phase conducted through source terms in the continuum equations. The proposed approach is orders of magnitude faster than a comparable approach based on the DSMC method. Note also that it may easily be extended to model heterogeneous condensation.

The following cluster-related processes are taken into account in the kinetic solver: (i) collisional dimer formation that uses theoretical temperature-based dimer formation rates defining the number of dimers created in each cell per time step, (ii) elastic monomer-cluster collisions that change the translational and internal energies of colliding particles, with energy transfer modeling using the Larsen-Borgnakke model, (iii) inelastic monomer-cluster collisions that result in monomer sticking, (iv) cluster-cluster coalescence simulated with a conventional DSMC collision algorithm based on the majorant frequency scheme, and (v) evaporation of monomers from clusters based on the RRK model.

The new model was found to reproduce well the known theoretical dimer formation equilibrium constants for two gases under consideration, argon and water. Water nozzle expansion was modeled with the stagnation pressure ranging from 1.5 bar to 8.3 bar, which corresponds to the average cluster size increasing from below 10 to over 300. The results on the terminal cluster were found sensitive to the cluster coalescence probability, with the average cluster size increasing significantly when this probability was increased from 0.25 to 1. Comparison with available experimental data have shown good agreement at lower pressures, and somewhat worse agreement at the highest pressure under consideration, where no visible bimodal size distribution structure was noticed in the calculations.

VI. Acknowledgments

The authors are extremely thankful to Prof. Udo Buck for his support and patience in explaining experimental setup and data, and providing additional data on cluster size distributions, Dr. Matthew Braunstein for his help with water binding energy analysis, and Dr. Y. Scribano for providing additional data for water dimer equilibrium constant and heat capacity. The work was supported by the Air Force Office of Scientific Research.

References

[1]Simmons, F.S. Rocket Exhaust Plume Phenomenology, The Aerospace Corporation Aerospace Press Series, Published by AIAA, 2000, 286p.

[2]R. T. V. Kung, L. Cianciolo, and J. A. Myer, "Solar Scattering from Condensation in Apollo Translunar Injection Plume," AIAA J. 13 (4), 432-437 (1975)

[3]Prandtl 1936 Atti del Convegno Volta, 1st edn., vol. XIV. Roma: Reale Academia D'Italia.

[4]X. LUO, G. LAMANNA, A. P. C. HOLTEN, M. E. H. van DONGEN, Effects of homogeneous condensation in compressible flows: Ludwieg-tube experiments and simulations, J. Fluid Mech. (2007), vol. 572, pp. 339-366.

[5]F. Abraham, *Homogeneous Nucleation Theory: The Pretransition Theory of Vapor Condensation* (Academic Press, New York, 1974).

[6]J. E. McDonald, Am. J. Phys. **31**, 31 (1963).

[7]Perrell, E.R., W.D. Erickson, and G.V. Candler, "Numerical Simulation of Nonequilibrium Condensation in a Hypersonic Wind Tunnel," Journal of Thermophysics and Heat Transfer, Vol. 10, No. 2, pp. 277-283, Apr.-June 1996.

[8]A.G. Gerber, "Two-Phase Eulerian/Lagrangian Model for Nucleating Steam Flow," Journal of Fluids Engineering, JUNE 2002, Vol. 124 465–475

[9]Jiangbo Qian, Zhonghe Han, Liansuo An, Unsteady Numerical Study on Steam Spontaneous Condensation in a Turbine Cascade, 3rd IEEE Conference on Industrial Electronics and Applications, 2008 720-722.

[10]Gyarmathy, G. 1976, Condensation in Flowing Steam, Two-Phase Steam Flow in Turbines and Separators, M. J. Moore and C. H. Sieverding, ed., Hemisphere, pp. 127-189.

[11]J.D. Chenoweth, K.W. Brinckman, J.J. York, G. Feldman, S.M. Dash, Progress in Modeling Missile Fuel Venting and Plume Contrail Formation,AIAA 2007-1012.

[12]D. P. Brown, J. Jokiniemi, and T. Valmarin, Computationally efficient modelling of multidimensional flui/aerosol processes, J. Aerosol Sci., Vol.28 pp, S323-S324, 1997

[13]Rubin, S. G., and Tannehill, J. C. (1992) "Parabolized/Reduced Navier-Stokes Computational Techniques", Annual Review of Fluid Mechanics. v 24, pp. I 17-144.

[14]J. Pusykiewicz, A. Kallaur, P. Smolarkiewiecz, Semi-Lagrangian modelling of tropospheric ozone, Tellus, Vol.49B, 1997, 231-248.

[15]R. Paoli, T. Poinsot AND K. Shariff, Testing semi-Lagrangian schemes for two-phase flow applications

[16]J. Zhong, M. Zeifman, S. Gimelshein, and D. Levin, "Direct Simulation Monte Carlo Modeling of Homogenous Condensation in supersonic Plumes," AIAA Journal **43**(8), 1784 (2005).

[17]G. A. Bird, *Molecular Gas Dynamics and the Direct Simulation of Gas Flows* (Clarendon Press, Oxford, 1994).

[18]C. Bobbert, S. Schutte, C. Steinbach, U. Buck, "Fragmentation and reliable size distributions of large ammonia and water clusters," Eur. Phys. J. D **19** pp. 183-192, 2002.

[19]A. Itkin and E. Kolesnichenko, *Microscopic Theory of Condensation in Gases and Plasma* (World Scientific, Singapore, 1997).

[20]H. Hettema and J. McFeaters, "The direct Monte Carlo method applied to the homogeneous nucleation problem," J. Chem. Phys. **105**, 2816 (1996).

[21]J. Soler, N. Garcia, O. Echt, K. Sattler, and E. Recknagel, "Microcluster growth: transition from successive monomer addition to coagulation," Phys. Rev. Lett. **49**, 1857 (1982).

[22]S. Toxvaerd, "Molecular-dynamics simulation of homogeneous nucleation in the vapor phase," J. Chem. Phys. **115**, 8913 (2001).

[23]M. I. Zeifman, J. Zhong, D. A. Levin, A Hybrid MD-DSMC Approach to Direct Simulation of Condensation in Supersonic Jets, *AIAA Paper 2004-2586* (2004).

[24]J. Zhong, M. Zeifman, D. Levin, Kinetic model of condensation in a free expanding jet, J. Thermophysics and heat transfer, 2006, Vol. 20, No. 1, pp. 41-51.

[25]A. Gallagher-Rogers, J. Zhong, D.A. Levin, "Simulation of Homogeneous Ethanol Condensation in Supersonic Nozzle Flows Using DSMC," AIAA Paper 2007-4159.

[26]J. Zhong and D. Levin, "Development of a Kinetic Nucleation Model for a Free-Expanding Argon Condensation Flow," AIAA Journal, 2007, Vol. 45, No. 4, pp. 902-911,

[27]B. Briehl and H. Urbassek, "Monte Carlo simulation of growth and decay processes in a cluster aggregation source," J. Vac. Sci. Tech.A, Vol. 17, No. 1, p. 256, 1999.

[28]S. Gratiy, J. Zhong, D.A. Levin, "Numerical Simulation of Argon Condensation with a Full Kinetic Approach in a Free-Expanding Jet," AIAA Paper 2006-3598.

[29]R.D. Levine, Molecular reaction dynamics, Cambridge University Press, 2005.

[30]R. Jansen, S. Gimelshein, M. Zeifman, I. Wysong, First-Principles Monte-Carlo Simulation of Homogeneous Condensation in Atomic and Molecular Plumes, AIAA Paper 2009-3745.

[31]N. Gimelshein, S. Gimelshein, A. Ketsdever, Thrust Augmentation in Solid Rocket Motors Using Beamed Microwave Energy, AIAA Paper 2009-4962.

[32]Toth, G. "General Code for Modeling MHD flows on Parallel Computers: Versatile Advection Code," Astrophysical Letters and Communications, Vol. 34, 1997, pp. 245-250.

[33]C. Borgnakke and P.S. Larsen, "Statistical collision model for Monte Carlo simulation of polyatomic gas mixture," J. Comp. Phys., 1975, Vol. 18, pp. 405-420.

[34]J. Zhong, M. I. Zeifman, and D. A. Levin, J. Thermophysics and Heat Transfer **20**(3), 517 (2006).

[35]J. F. Crifo, ICARUS, **84**, 414 (1990).

[36]M. Zeifman, B. J. Garrison, and L. V. Zhigilei, J. Appl. Phys. **92**, 2181 (2002).

[37]Y. Okada and Y. Hara, Earozoru Kenkyu **22**(2), 147 (2007).

[38]N. Ashgriz and J. Y. Poo, Coalescence and separation in binary collisions of liquid drops, Journal of Fluid Mechanics (1990), 221:183-204

[39]R. Kalus, J. Chem. Physics **109**(19), 8289 (1998).

[40]Y. Scribano, N. Goldman, R. J. Saykally, and C. Leforestier, J. Phys. Chem. A **110**(16), 5411 (2006).

[41]M.S. Ivanov and S.V. Rogasinsky, "Analysis of numerical techniques of the direct simulation Monte Carlo method in the rarefied gas dynamics," *Sov. J. Numer. Anal. Math. Modelling* **2** (6), 1988, pp. 453-465.

[42]S. Schütte and U. Buck, Int. J. Mass Spec. **220**, 183 (2002).